Morphology of Immiscible Polymer Blend Thin Films Prepared by Spin-Coating

Peng Wang and Jeffrey T. Koberstein*

Department of Chemical Engineering, Columbia University, MC4721, 500 West 120th Street, New York, New York 10027

Received February 18, 2004; Revised Manuscript Received May 11, 2004

ABSTRACT: The morphologies of spin-coated thin films of the immiscible polymer blend of polystyrene and poly(*tert*-butyl acrylate) (PS/PtBA) are characterized by X-ray photoelectron spectroscopy (XPS), Fourier transform infrared spectroscopy (FTIR), and scanning force microscopy (SFM) combined with selective dissolution. PS and PtBA are found to phase separate laterally in the thin films after spin-coating. The overall trend with blend composition is for PS islands to form when the PS:PtBA ratio is less than unity and for PtBA holes to form when the PS:PtBA ratio is larger than unity. The thickness of PS phases always exceeds that of the PtBA phases with both thicknesses increasing linearly with concentration of the spin-coating solution. The addition of P(S-*b*-tBA) diblock copolymer decreases the overall domain dimensions. After long annealing periods, PtBA is found to segregate preferentially to both the air−polymer interface and the polymer−substrate interface, effectively encapsulating PS droplet domains. A simple free energy model developed for the annealed specimens predicts a local free energy minimum as a function of PS droplet diameter, accounting for the observed stability of PS droplet phases and their very slow growth upon annealing. The surface tension of PtBA and the interfacial tension between PS and PtBA are shown to be critical parameters that affect the domain morphology in annealed PS/PtBA thin films.

Introduction

The morphological control of immiscible polymer blends is a topic of great interest because of the strong influence of phase geometry and dimensions on material properties and performance. There is a vast literature that describes how blend properties depend on morphology and how phase size and shape can be controlled by processing conditions.[1] In general, the morphological character of immiscible polymer phases is not an intrinsic thermodynamic function but is determined by the nonequilibrium nature of the processing operations employed for fabrication. In melt processing, nonequilibrium morphologies created in the melt are frozen in either by reactive processing[1c] or by subsequent cooling to the point of vitrification. In solvent-based processing, phase structures form during solvent evaporation, and their development is arrested at the point where solvent removal leads to vitrification. Polymer blends often undergo phase separation transitions during processing, starting out as a single phase melt or solution and separating into phases as the temperature is changed or solvent is removed. The possible morphologies obtainable through available processing technologies are almost without limit.

The focus of the current work is the morphology of thin films of immiscible polymer blends deposited onto solid substrates, in particular, those formed by spin-coating operations. Spin-coating is employed broadly for the fabrication of thin polymer films because of the precise control of thickness it affords by simply changing the rotational velocity or the polymer solution concentration.[2,3] If the spin-coating solution consists of two or more immiscible polymers dissolved in a common solvent, the film will usually undergo phase separation to form separate domains upon solvent evaporation. The phase separation process, however, is highly constrained for thin polymer blend films. The film thickness can be orders of magnitude smaller than the micron scale phase dimensions usually observed in bulk phase separation, and the effects of two interphases must be considered: the interphase between the polymer solution and air and the interphase between the polymer solution and the substrate. For thin films, the interfacial energies associated with these interphases can be of similar magnitudes as the bulk free energy and therefore can have a profound effect on the critical conditions for phase stability. Furthermore, thin film blend morphology is also dependent on a number of interfacial phenomena, including preferential wetting and dewetting of certain constituents on the substrate and preferential segregation of one constituent to the air−polymer interface. The nonequilibrium morphologies frozen in during spin-coating of immiscible polymer blends are thus dependent on a complex competition of a number of physical phenomena.

Recent research has attempted to relate phase morphology in thin polymer blend films to the mechanisms of structure formation, particularly for solvent-based film casting processes such as spin-coating. Walheim et al.[4] used atomic force microscopy (AFM) and selective dissolution to study morphology in polystyrene/poly(methyl methacrylate) (PS/PMMA) thin films. Domain structures and surface topography were found to depend on both the energies of component interactions with the substrate and the energies of interactions of the polymers with the solvents. Ton-That et al.[5−7] also examined the morphologies of PS/PMMA thin films using AFM and X-ray photoelectron spectroscopy (XPS). Because the technique of selective dissolution of one phase was not applied, only surface composition and morphological information was obtained. They concluded that the

* Corresponding author: e-mail jk1191@columbia.edu; tel (212) 854-3120; Fax (212) 854-3054.

10.1021/ma049664+ CCC: $27.50
Published on Web 06/29/2004

Table 1. Characteristics of Polymers Used

polymer notation	M_n	M_w/M_n	T_g (°C)
PS21	20800	1.07	102
PtBA14	14400	1.06	39
P(S7-*b*-tBA6)	7000−6400	1.33	NA
P(S206-*b*-tBA202)	206200−201800	1.20	NA

surface morphology could be explained in terms of the relative solubility of the two polymers in the solvent and differences in the ability of PMMA and PS to wet the substrate. The size of surface features was found to increase with the total concentration of the casting solution. Tanaka et al.[8] observed that surface structure of PS/PMMA films changed remarkably with the film thickness. For example, a 10.2 nm thick PS/PMMA film did not show any distinct phase-separated structure, while a 6.7 nm film exhibited domains with a size of a few hundred nanometers. Morphological changes were attributed to the film thickness dependence of both the interaction parameter and the degree of entanglement among polymer chains.

Thin film morphology can be altered by thermal annealing applied after spin-coating. The changes in domain structures during annealing provide insight into the factors and phenomena that control thin film blend morphology. Wang et al.[9−11] investigated the evolution of morphology in thin films of deuterated PMMA and poly(styrene-*ran*-acrylonitrile) (SAN) upon annealing. They defined four regimes of behavior dependent on film thickness. Unique pathways for phase evolution were assigned for each behavioral regime, even though the final morphologies obtained in different regimes were sometimes identical.

This paper investigates the morphologies for thin films prepared from immiscible mixtures of polystyrene with poly(*tert*-butyl acrylate) (PtBA). The PS/PtBA blend system was selected for study because it has several important distinctions from previous systems studied, especially the popular PS/PMMA system. Because PtBA has a much lower T_g than that of PMMA or PS, the time scales required for observing morphological changes caused by annealing are significantly shorter. PtBA also segregates preferentially to both the polymer−air interface and the interface with a silicon wafer. The former effect occurs because PtBA has a lower surface tension than PS by virtue of the *tert*-butyl side chains, while the latter effect is related to interactions between the ester group in PtBA and the silicon oxide surface on the substrate. In the case of the previously studied PS/PMMA system, PMMA segregates preferentially to the substrate; however, PS segregates preferentially to the air−polymer interface if the molecular weights are similar. We report the dependence of PS/PtBA thin film morphology on spin-coating solution composition, film thickness, annealing conditions and added P(S-*b*-tBA) diblock copolymer. A simple free energy model is proposed to explain the apparent metastable morphologies observed in the annealed specimens.

Experimental Section

Materials. PS, PtBA, and poly(styrene-*b*-*tert*-butyl acrylate) P(S-*b*-tBA) were purchased from Polymer Source Inc. and used as received. Their characteristics are listed in Table 1. In the nomenclature adopted, the numbers after the polymer designation indicate the nominal number-average molecular weight (M_n) of the polymer or block copolymer sequence in kDa. The glass transition temperatures (T_g) of PtBA and PS were determined using a differential scanning calorimeter (Q100, TA instruments, Inc.).

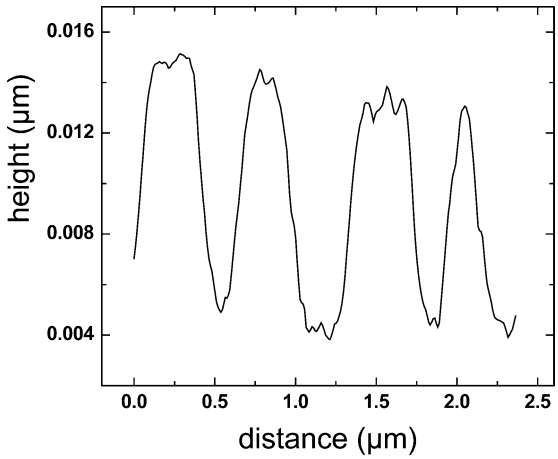

Figure 1. Height profile of a typical spin-coated film.

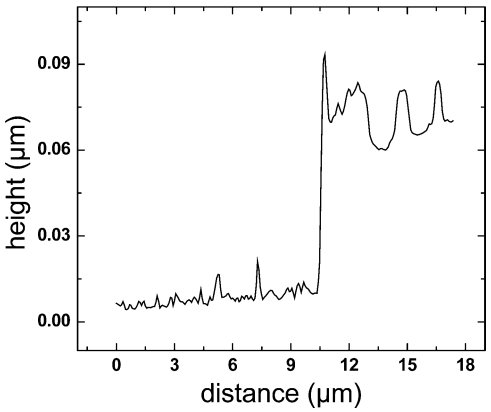

Figure 2. Height profile of a typical scratched film.

Sample Preparation. Polymer blend thin films were prepared by spin-coating solutions containing the appropriate amounts of polymers for 40 s at 3000 rpm using a spin processor (WS-400A-6NPP/LITE) manufactured by Laurell Technologies Corp. Solvents were analytic grade toluene, methanol, and cyclohexane (Aldrich). The total polymer concentration in the solutions was 0.01 g/cm^3 unless otherwise noted. Silicon wafers (Wafer World, Inc.) were cut into 1 cm × 1 cm squares and washed successively with acetone and deionized water. Substrates were further cleaned at 90 °C in a piranha solution of 70% (v) H_2SO_4 and 30% (v) H_2O_2. After soaking for 15 min in piranha solution, the substrates were washed with deionized water and dried with compressed nitrogen (Tech. Air). To test the stability of the structures formed, some films were annealed in a vacuum oven at 110 °C, above the glass transition temperatures of any polymers used in this study. Samples were cooled to room temperature under vacuum after annealing.

Scanning force microscopy (SFM) measurements using the AutoProbe CP Research probe head (Veeco Instruments) were performed in noncontact mode (NCM-AFM) to investigate the surface structure of polymer blend thin films. Silicon cantilevers (dLevers) were supplied as a group of four different cantilevers on each chip. Cantilever A with the smallest force constant was used in all measurements in order to minimize surface damage caused by the tip. IP Autoprobe Image (Veeco Instruments) software was used to analyze the images. Most as-cast films investigated in this article exhibit surface features that can be described as either islands or holes. Figure 1 shows a height−distance profile of a typical sample surface. Absolute feature heights were obtained by scratching the film with a tweezers and then measuring the height profile with NCM-AFM. Figure 2 presents an example of a typical height profile curve of a sample after scratching.

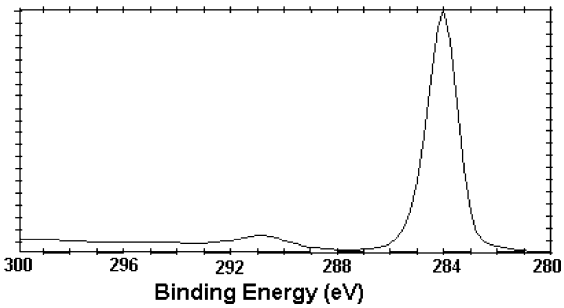

Figure 3. High-resolution C_{1s} spectrum of PS.

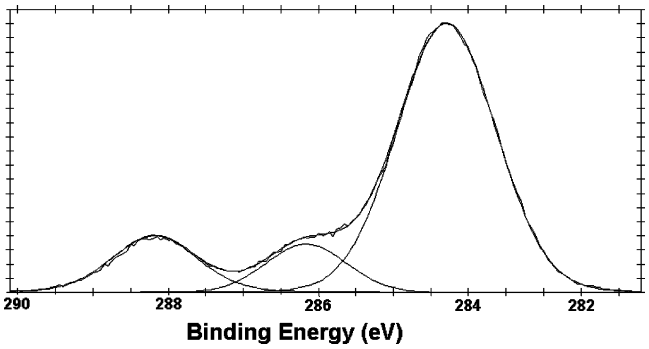

Figure 4. High-resolution C_{1s} spectrum of PtBA.

Although SFM is a powerful tool for characterizing the surface topography of polymer films, it is difficult to distinguish different chemical species by SFM alone. Lateral force microscopy (LFM) can provide additional insight, but LFM is subject to artifacts that can be misleading. An alternative is to combine AFM measurements with contrast enhancement by selective dissolution, a technique that was previously applied[4,12] to study domain structures in blend thin films. In this article, methanol and cyclohexane were employed as selective solvents for etching PtBA and PS, respectively. NCM-AFM images were taken before and after solvent etching to better examine domain structures. Fourier transform infrared (FTIR) spectra were recorded with a Magna-IR 560 (Thermo Nicolet) spectrometer.

X-ray photoelectron spectroscopy (XPS) data were collected with a Perkin-Elmer PHI model 5500 X-ray photoelectron spectrometer using a monochromatic Al Kα X-ray source. Typical operating conditions were 15 kV and 350 W for the Al X-ray source, 23.5 eV pass energy for high-resolution C_{1s} scans, and an operating pressure of approximately 5×10^{-9} Torr. High-resolution C_{1s} spectra were decomposed into various contributions from carbon atoms that experience different chemical shifts due to their different chemical environments. Figures 3 and 4 show C_{1s} spectra of the PS21 and PtBA14, respectively. In the PS spectrum, the small peak with binding energy around 291 eV is the so-called "shake-up" satellite associated with the known $\pi-\pi^*$ transition for aromatic systems. The three carbon contributions in the spectrum of PtBA14 correspond to O═*C*−O, O−*C*−C, and the other remaining carbons, from left to right, respectively. The area fraction of the O═*C*−O contribution is 14.4%, which agrees well with the value 14.29% (i.e., 1 out of 7) expected from the structure of PtBA. We define R_a as the area fraction of the O═*C*−O peak in the C_{1s} spectrum and R_m as the molar fraction of styrene at the surface:

$$R_m = \frac{\text{no. of PS monomers}}{\text{no. of PS monomers} + \text{no. of PtBA monomers}} \quad (1)$$

Each *tert*-butyl acrylate repeat unit has seven carbon atoms, one of which is O═*C*−O. Each styrene molecule has eight carbon atoms. Blends of PtBA and PS, therefore, have the following relationship between R_a and R_m:

$$R_a = \frac{(\text{no. of PtBA monomers}) \times 1}{(\text{no. of PtBA monomers}) \times 7 + (\text{no. of PS monomers}) \times 8} = \frac{1 - R_m}{7(1 - R_m) + 8R_m} \quad (2)$$

The C_{1s} peak from O═*C*−O is chosen for the calculation because its binding energy is well separated from that of the other C_{1s} peaks. Neglecting the small density difference between the two polymers, the molar fraction R_m can be transformed into R_S, the area fraction of PS at the surface, by applying the following formula:

$$R_S = \frac{R_m \times M_n \text{ of styrene}}{(1 - R_m) \times M_n \text{ of } \textit{tert}\text{-butyl acrylate} + R_m \times M_n \text{ of styrene}} \quad (3a)$$

$$= \frac{R_m \times 104}{(1 - R_m) \times 128 + 104 \times R_m} \quad (3b)$$

From eqs 2 and 3b, R_S can be written as a function of R_a:

$$R_S = \frac{104 - 728R_a}{104 + 296R_a} \quad (4)$$

It should be noted that the value of R_S thus obtained from XPS is not necessarily equal to that obtained from NCM-AFM measurements enhanced by selective solvent etching. XPS provides characterization of only the top few nanometers of a material. Thus, it is possible that a very thin layer of PtBA covering polystyrene domains will be detected by XPS but that removal of this layer by solvent etching will not significantly alter the NCM-AFM images.

Results and Discussion

The ultimate domain structure obtained for thin, spin-coated films of immiscible PtBA/PS blends, and other binary blend systems, is determined by a complex interplay of many factors and processes, including solubility differences between the two blend constituents in the solvent used, the interfacial tension between the two polymers, and preferential segregation of one of the polymers to the silicon−polymer and polymer−air interfaces, a process governed by surface tension differences. As the solvent evaporates, the solution of the two polymers will reach a critical concentration at which a single phase is no longer stable, and macrophase separation is expected to occur. Although the equilibrium morphology is two large separate phases, the spin-coating process is too rapid for equilibrium to be obtained, and some intermediate morphology is usually frozen in by vitrification of one or both of the polymers. For the case of thin films, this process is further complicated by preferential surface segregation or formation of a wetting layer at either the air−polymer or polymer−substrate interfaces. Previous studies on thin films of polymer blends have helped to elucidate some aspects of morphology development during spin-coating.[4−11]

The primary goal of the present work is to provide additional information about the morphologies produced in spin-coated films of immiscible polymer blends by studying the system PTBA/PS. The PtBA/PS system was selected for study because PtBA is expected to preferentially wet the substrate and to segregate pref-

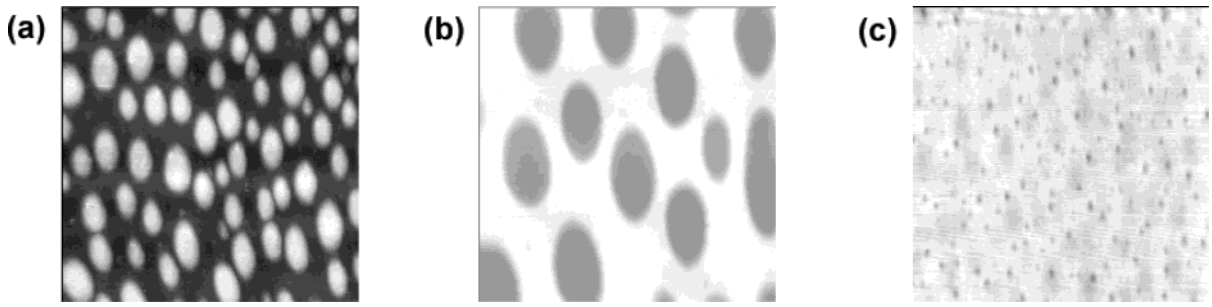

Figure 5. NCM-AFM topographic images of the PS/PtBA films (scan size: 4 μm × 4 μm): (a) PS:PtBA = 1:4; (b) PS:PtBA = 1:1; (c) PS:PtBA = 4:1.

erentially to the air−polymer interface. Because PS will not wet a PtBA surface (based upon the known dewetting of PS on PMMA)[13,14] and is not favored at the surface, equilibrium considerations would suggest a morphology consisting of PS phases surrounded by a PtBA matrix. Any PS domains that form would naturally try to assume a spherical shape in order to minimize the interfacial area (i.e., interfacial energy) with PtBA; however, this would cause them to protrude from the surface and would be balanced by an increase in the surface free energy associated with the corresponding increase in area of the air−polymer interface. PtBA has a glass transition temperature near room temperature, but PS has a glass transition temperature above room temperature and would be expected to vitrify at some critical solvent concentration, freezing in some nonequilibrium morphology.

While it would be preferable to track the kinetics of structure formation during spin-coating in order to fully eludicate the mechanisms of morphology generation, the approach taken in this first study is to examine how certain spin-coating variables influence the morphology obtained after spin-coating. The first three sections of experimental results examine how the morphology of spin-coated thin films of PtBA/PS blends is affected by changes in the spin-coating solution composition and concentration, which controls the film thickness, and by addition of a poly(tBA-*b*-S) diblock copolymer. The fourth section of the paper illustrates how the as-cast structures evolve during annealing and includes a free energy model to account for the quasi-equilibrium morphologies obtained after long annealing times.

A. Effect of Spin-Coating Solution Composition. The first part of the study focuses on characterizing thin films of immiscible PS/PtBA blends prepared by spin-coating from the mutual solvent, toluene. The objective is to understand how the morphology varies with blend composition. Topographic images of three typical samples from NCM-AFM measurements are shown in Figure 5. The bright/dark areas in the images correspond to thicker/thinner regions, respectively. Islandlike features with a diameter of about 0.5 μm are observed at the surface for the lowest concentration of PS (PS:PtBA = 1:4) and transform into holelike features with a diameter of about 0.8 μm as the PS:PtBA ratio is increased to 1:1. The diameter of the holes decreases significantly to about 0.05 μm when the ratio increases to 4:1. Films with other mass ratios (PS:PtBA = 3:7 and 7:3) were also prepared and characterized by SFM. The overall trend is for islands to form when the PS:PtBA ratio is less than one and for holes to form when the PS:PtBA ratio is larger than or equal to one. Islands or holes often show collective orientation that is perhaps related to the flow field in spin-coating, but these effects were not studied systematically.

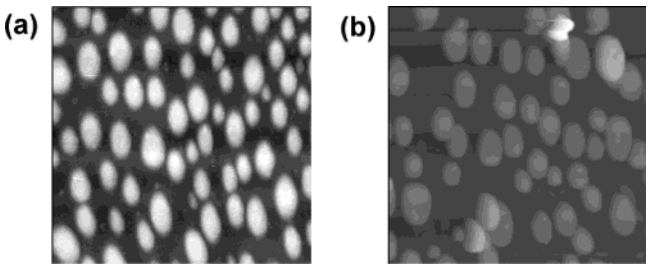

Figure 6. NCM-AFM topographic images of the PS/PtBA films (PS:PtBA = 1:4; scan size: 4 μm × 4 μm): (a) original film; (b) after being washed with methanol.

Methanol, a solvent for PtBA and nonsolvent for PS, was used to develop surface contrast by selective extraction of PtBA. The value of R_a obtained from XPS measurements decreases significantly during rinsing with methanol, indicating removal of PtBA from the surface. In Figure 6, NCM-AFM topographic images of a film (PS:PtBA = 1:4) before and after rinsing with methanol are compared. Qualitatively, the topography of the film does not change much after rinsing with methanol for 5 min. However, quantitative analysis reveals important differences. Line scans corresponding to the two pictures in Figure 6 are given in Figure 7. Although the diameters of the islands do not significantly change after methanol exposure, the feature heights increase significantly from about 15 to 75 nm, indicating that the film is laterally phase separated, with the darker (thinner) regions in Figures 5 and 6a being composed primarily of PtBA. Silicon peaks, which do not exist in XPS spectra for the as-cast films, appear after rinsing, suggesting that the PtBA domains, which were washed away during rinsing, were originally in contact with the silicon substrate.

NCM-AFM images and line scans for a PS:PtBA = 1:1 sample are shown in Figures 8 and 9, respectively. The surface retains the original holelike features after washing with methanol. Films with different compositions (PS:PtBA = 3:7, 7:3, and 4:1) were prepared and characterized with the same method. Good repeatability was observed: methanol was always found to etch the thinner regions until the silicon substrate was exposed. In other words, methanol selectively etches the holes if the original film shows holelike features or the matrix regions if the original film shows islandlike features. These observations indicate that the thicker regions visible in the NCM-AFM images are PS-rich regions.

NCM-AFM images were analyzed to obtain the surface area fractions, $R_{F,}$ occupied by the PS domains. The results are given in Table 2. XPS measurements were

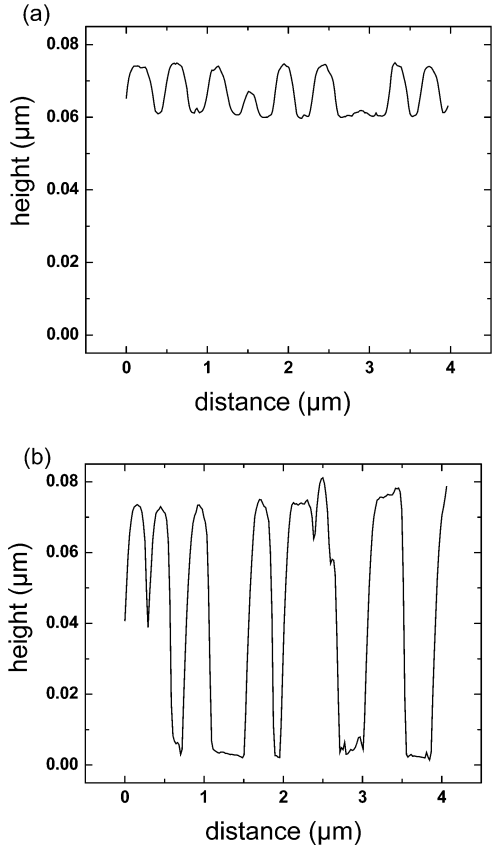

Figure 7. Typical NCM-AFM line scans of the surface of PS/PtBA film (PS:PtBA = 1:4): (a) scan on the original film; (b) scan on the film after being washed with methanol. For clarification, absolute height is used, and the surface of substrate is set as the zero point.

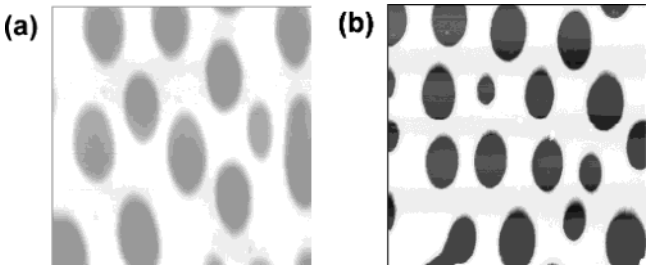

Figure 8. NCM-AFM topographic images of the PS/PtBA film (PS:PtBA = 1:1; scan size: 4 μm × 4 μm): (a) original film; (b) after being washed with methanol.

also applied to obtain the PS surface area fractions, R_S. R_S is significantly lower than both R_F and the mass fractions of PS in the mixture, suggesting that PtBA segregates preferentially to the air−polymer interface. Surface segregation of PtBA is expected because its surface tension is lower than that of PS (see Table 4). Because of the roughness of the surface associated with the thin film domain structure, characterization of the spatial distribution of PtBA at the surface with a technique such as angle-dependent XPS is not viable. It is not known therefore whether PtBA forms a complete wetting layer or a gradient at the surface. Regardless of the actual surface structure, it can be concluded that the total amount of PtBA located at the surface is small because there is no detectable change in the height of PS domains after selective etching with methanol, even though the surface concentration of PtBA, within the XPS sampling depth of 7−10 nm, drops essentially to zero after etching.

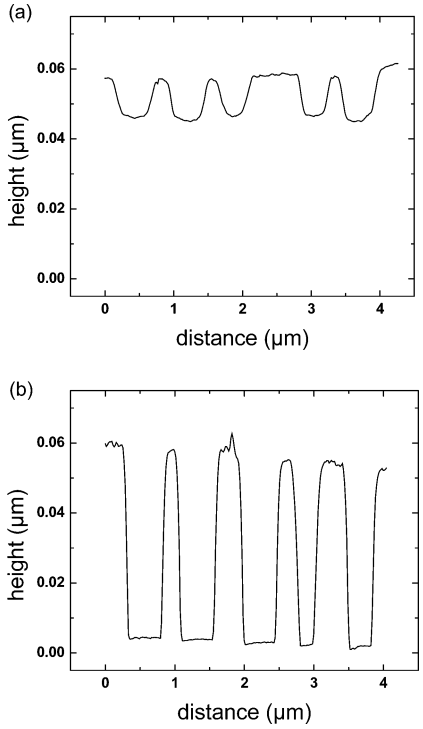

Figure 9. Typical NCM-AFM line scans of the surface of blends film (PS:PtBA = 1:1): (a) scan on the original film; (b) scan on the film after being washed with methanol.

Table 2. Surface Area Fractions of PS Phase

composition ratio PS:PtBA (wt:wt)	R_F from AFM	R_S from XPS
1:4	37.0 ± 3.2	5 ± 3.0
1:1	52.0 ± 4.4	18 ± 2.5
4:1	88.4 ± 5.0	30 ± 4.0

Table 3. Effect of Spin-Coating Solution Concentration on Morphological Shape Factors

concn [g/cm^3]	h_2 [nm]	h_2/h_1	$(h_2R_F)/h_1$
2×10^{-3}	26	2.56	1.331
5×10^{-3}	48	1.59	0.986
1×10^{-2}−4×10^{-2}	58−227	1.32	0.713

Table 4. Surface Tension of PS and PtBA[19,20] [mJ/m^2]

polymer	surface tension	dispersive component	polar component
PS	41.5	36.2	5.3
PtBA	33.7	30.4	3.3

The value of R_F determined from NCM-AFM measurements is larger than the corresponding mass fraction of PS in the polymer mixture, indicating that the projected area fraction of PS domains is larger than expected from the film composition. There are two possible explanations for this behavior: PtBA could be trapped as inclusions within the PS domains, thereby increasing the overall area fraction of PS domains, or PtBA could be located beneath the PS domains if it adsorbs preferentially on the substrate. Trapped inclusions were reported in previous studies of the PS/PMMA system,[4−8] providing some support for the former explanation. The results of solvent etching experiments are contrary to the latter explanation because the entire structure would be expected to lift off upon exposure to methanol if a continuous PtBA wetting layer were in contact with the silicon substrate. It is worthwhile to mention that when etched with cyclohexane, a selective solvent for PS, the film is destroyed, consistent with the

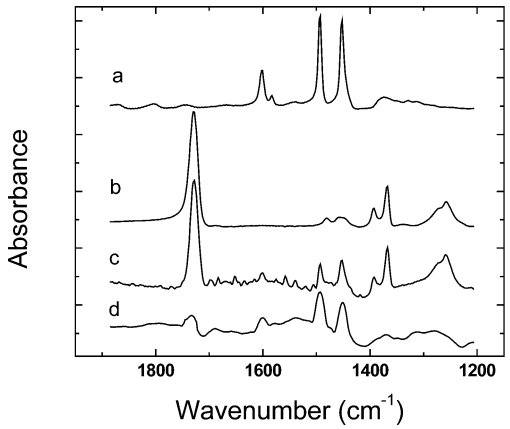

Figure 10. FTIR spectra: (a) PS film; (b) PtBA film; (c) blend film before washing; (d) blend film after washing with methanol.

idea that some polystyrene is in direct contact with the silicon substrate in as-cast films. This result might be expected if the spin-coating process is too rapid to allow PtBA to form the expected wetting layer on the silicon substrates. Alternatively, it is also possible that the methanol contact time was too short to allow for complete dissolution of a PtBA layer underlying PS domains. The measurements of RF therefore indicate that some PtBA remains in the films after selective etching with methanol, although the data do not indicate the location of residual PtBA.

FTIR analysis also indicates that the as-cast films contain residual PtBA after selective methanol etching. Infrared analysis samples the entire film, and the absorption band at 1730 cm^{-1} is associated exclusively with the carbonyl stretching vibration from PtBA. The infrared spectrum in Figure 10 illustrates that PtBA does remain in the film after etching.

The existence of residual PTBA within the as-cast films was further confirmed with additional XPS experiments combined with ion milling. The as-cast films were etched by methanol until PtBA was not detectable by XPS, indicating the absence of PtBA within the XPS sampling depth. The concentration of PtBA at the surface (indicated by the height of the C_{1s} peak from O═*C*−O) was then measured again after an arbitrary amount of polymer was removed from the surface by sputtering with an ion gun inside the XPS test chamber. The O═*C*−O content increased after milling, indicating that the films do contain residual PtBA after methanol etching. The location of PtBA within the films can in principle be investigated by XPS experiments performed as a function of the milling time; however, we have not performed such experiments because they require considerable care and their interpretation for rough samples is not straightforward. Unfortunately, it is not possible from the present data to determine whether the residual PtBA found in as-cast blend films after methanol etching is present as inclusions within PS domains or as a layer underlying the PS domains.

B. Effect of Spin-Coating Solution Concentration. The second variable examined was the film thickness, adjusted by varying the concentration of the spin-coating solution. Polymer solutions with total polymer concentrations of 2×10^{-3}, 5×10^{-3}, 1×10^{-2}, 2×10^{-2}, 3×10^{-2}, and 4×10^{-2} g/cm^{-3} were prepared, keeping the mass ratio of PS to PtBA fixed at 1:1. Two morphological parameters, h_2 and h_1, defined as the

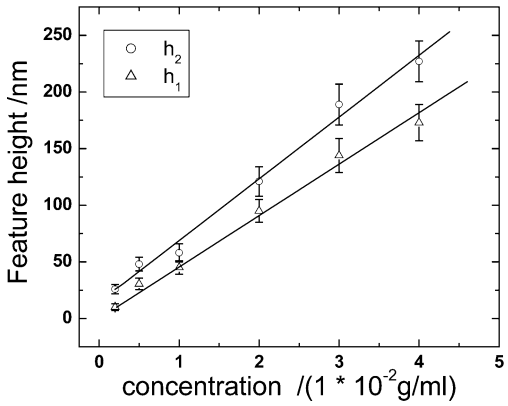

Figure 11. Dependence of feature height on the concentration of coating solution.

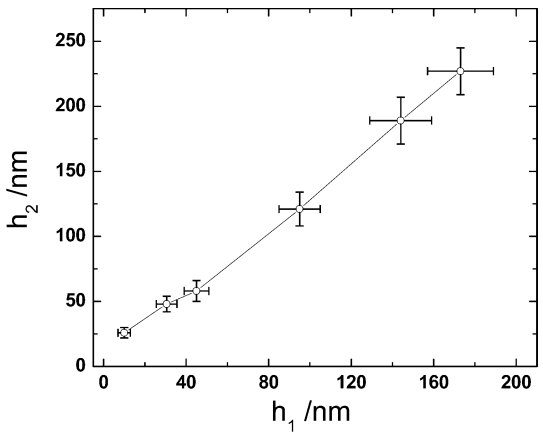

Figure 12. Relationship between h_2 and h_1.

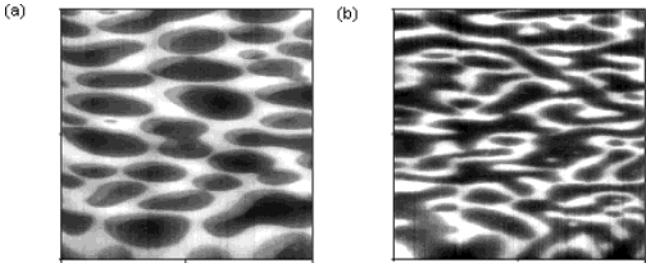

Figure 13. NCM-AFM images of the PS/PtBA films (PS:PtBA = 1:1; scan size: 5 μm × 5 μm) made from solution with different concentration: (a) total polymer weight concentration = 5×10^{-3} g/cm^{-3}; (b) total polymer weight concentration = 2×10^{-3} g/cm^{-3}.

height of the PS domains and the PtBA domains, respectively (see Figure 17a), were determined from analysis of the NCM-AFM images. Three samples were prepared for each concentration, and five line profiles were recorded for each sample. The effect of concentration is to increase the average h_2 and h_1 values as shown in Figure 11. Figure 12 illustrates the relationship between h_1 and h_2. When h_2 exceeds 58 nm, h_1 increases linearly with h_2. All of the films that show this linear behavior were found to exhibit holelike features in the NCM-AFM images. The diameter of the holes increases monotonically with thickness, a phenomenon that has also been observed in other binary mixtures.[7,15] However, as h_2 decreases below 58 nm, corresponding to solution concentrations below 1×10^{-2} g/cm^{-3}, the linearity between h_1 and h_2 is lost, suggesting that films may exhibit different morphologies within this region. More direct evidence is available from examination of

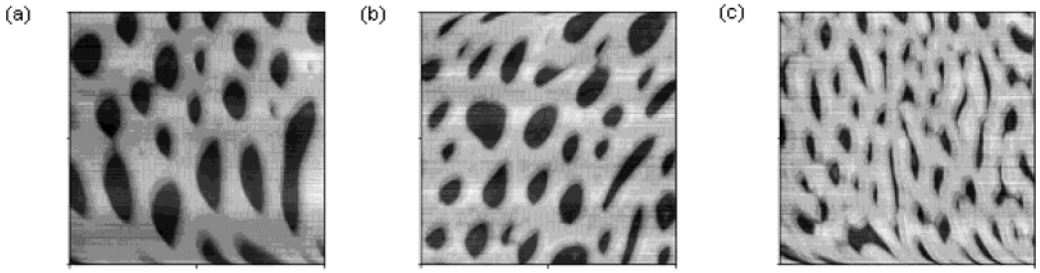

Figure 14. NCM-AFM topographic images of blend film with adding of block polymer P(S7-*b*-tBA6) (scan size: 5 μm × 5 μm): (a) PS:PtBA:P(S7-*b*-tBA6) = 5:5:1; (b) PS:PtBA:P(S7-*b*-tBA6) = 5:5:2; (c) PS:PtBA:P(S7-*b*-tBA6) = 1:1:1.

the NCM-AFM images. Figure 13 shows typical samples that were prepared from 5×10^{-3} and 2×10^{-3} g/cm^{-3} solutions. The image for the film made from a 5×10^{-3} g/cm^{-3} solution shows a structure of interconnected holes while the film prepared from 2×10^{-3} g/cm^{-3} solution has a lacy networklike structure reminiscent of that reported for spinodal decomposition of PMMA/poly(styrene-*ran*-acrylonitrile) blends.[16]

The effect of concentration (i.e., film thickness) on morphology can be further elucidated by calculating the two morphological shape factors, h_2/h_1 and $(h_2R_F)/h_1$, listed in Table 3. h_2/h_1 is the ratio of heights of the PS and PtBA domains, respectively, and provides an indication of the roughness of the surface. The ratio $(h_2R_F)/h_1$ reflects whether pure phases extend completely between the substrate and the polymer−air interface. If this is the case, $(h_2R_F)/h_1$ has a value of about 0.5, equivalent to the mass fraction of PS in the blends. The fact that $(h_2R_F)/h_1$ is found to exceed 0.5 indicates that the PS phase does not extend completely between the substrate and the polymer−air interface. That is, PtBA must exist as inclusions within the PS phase, as a layer beneath the PS phase, as a layer on top of the PS phase, or in all three locations. The decrease in $(h_2R_F)/h_1$ with concentration may be a kinetic effect. That is, a relatively larger percentage of PtBA is able to move to the air−polymer and substrate−polymer interfaces during spin-coating when the polymer concentration, and thus the viscosity, is lower.

C. Effects of Diblock Copolymer Addition. The third goal of this investigation is to demonstrate the effects of block copolymer addition on the morphology of polymer blend thin films. It is well-known that the addition of a diblock copolymer comprising blocks of the two homopolymers may significantly change the morphology and bulk properties of a polymer blend, in part due to their effect on interfacial tension.[1c,17,18] To investigate the effects of diblock copolymer addition on the morphology of thin films made from immiscible blends, two block copolymers of different molecular weights, P(S7-*b*-tBA6) and P(S206-*b*-tBA202), were added into blends of PS21 with PtBA14. The total polymer weight concentration in the spin-coating solution was fixed at 1×10^{-2} g/cm^3. NCM-AFM images for these ternary blend films are shown in Figures 14 and 15. As P(S7-*b*-tBA6) is added, the holes become smaller and less symmetric, and the distance between holes decreases correspondingly. The changes become more evident with an increase in block copolymer concentration. Block copolymer addition leads to a decrease in size of the holes because the associated increase in interfacial area is offset by a reduction in interfacial tension.[18] The radius of curvature of the holes can be smaller for a lower interfacial tension according to the La Place equation.[19] Block copolymer addition also appears to make the phases more deformable by the shear forces involved with spin-coating, as might be expected with a decrease in interfacial tension.

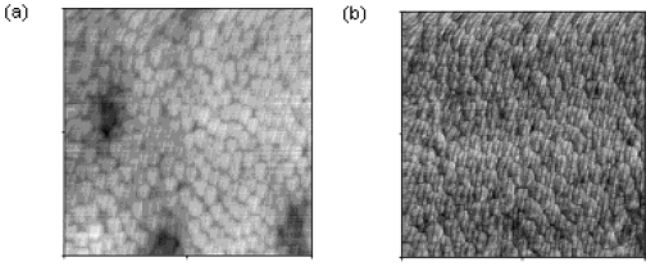

Figure 15. (a) NCM-AFM topographic and (b) phase images of blend film with adding of block polymer P(S206-*b*-tBA202) (scan size: 5 μm × 5 μm). PS:PtBA:P(S206-*b*-tBA202) = 1:1:1.

Addition of P(S206-*b*-tBA202) causes a marked change in the topography of the films, as shown in Figure 15. A distinct microemulsion structure is apparent for these films. Emulsion structures are also observed in the corresponding phase image (Figure 15b) at the surface of both the thinner and thicker regions. The microemulsion structures observed are caused by dissolution of homopolymers inside of the corresponding blocks of the higher molecular weight copolymer. Consequently, unlike the result for films containing P(S7-*b*-tBA6), the topographies of films containing P(S206-*b*-tBA202) are dominated by the intrinsic morphology of the diblock copolymer. The size of the microemulsions can be tuned by varying the molecular weight of the diblock copolymer as long as the homopolymer still dissolves within the copolymer. Theoretically, the microemulsion dimensions can also be adjusted by varying the homopolymer-to-copolymer ratio. These preliminary experiments illustrate that diblock copolymer addition is an effective method for controlling the morphology of polymer blend thin films.

D. Effects of Annealing. The stability of nonequilibrium blend morphologies frozen in during spin-coating was tested by vacuum-annealing thin films at 110 °C. Films with PS to PtBA ratios in the range of 1:4 to 4:1 were investigated. In all cases, annealing led to the formation of PS droplets, given sufficient time (Figure 16a). Extraction with cyclohexane, a selective solvent for PS, leads to the craterlike structure evident in Figure 16b. The NCM-AFM image of rinsed films suggests that the PS phases were originally covered with a PtBA layer that was too thin to resist diffusion of cyclohexane into the underlying PS droplets. The crater structure implies that large, nearly spherical PS domains originally protruded from the surface and were removed by solvent extraction. These domains rested on a wetting layer of PtBA, which remains after cyclohexane etching. It is well-known that the minority

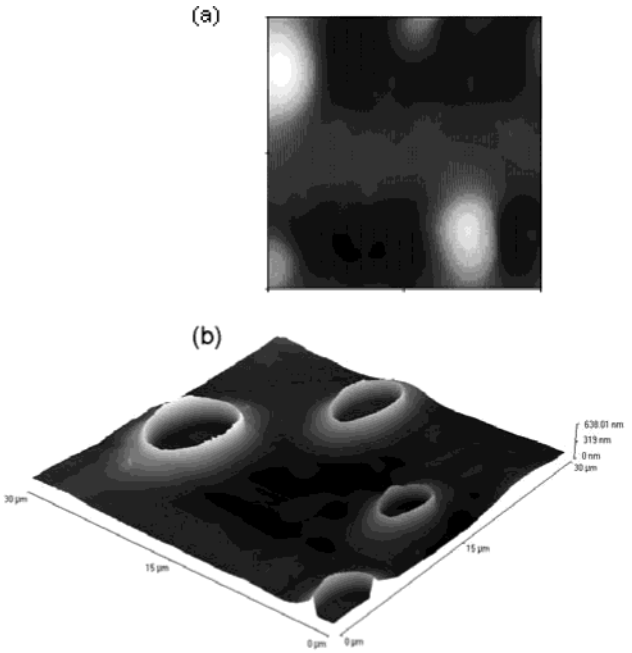

Figure 16. NCM-AFM topographic images for the PS/PtBA films (PS:PtBA = 1:1; scan size: 30 μm × 30 μm) after annealing at 110 °C for 4320 min: (a) before rinsing with cyclohexane; (b) after rinsing.

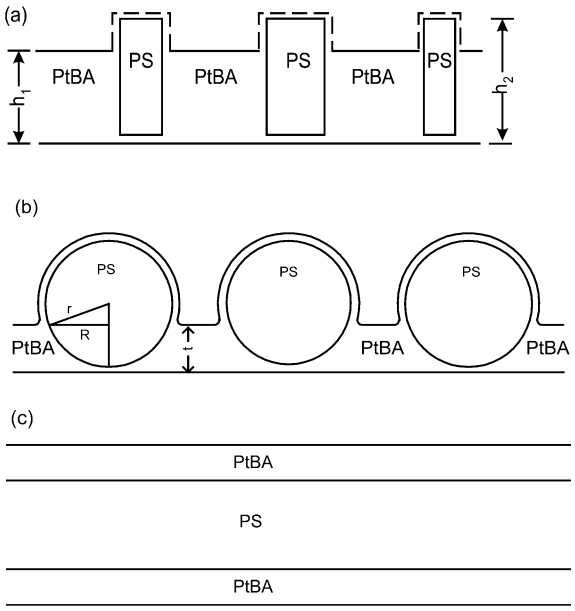

Figure 17. Schematic pictures of domain structure in thin films: (a) the domain structure in thin films after spin-casting; (b) the domain structure in thin films after annealing; (c) a hypothetical multilayer structure.

component in a polymer blend tends to form discontinuous inclusions in the bulk in order to minimize interfacial energy. In contrast, PS is always found to form a discontinuous phase in the annealed PS/PtBA thin films investigated herein, regardless of which polymer is the minority component.

The parameter R_a determined by XPS increases immediately after annealing and reaches ~14% after 5−10 min. Theoretically, R_a should be 14.29% for pure PtBA. The XPS measurement therefore indicates that it takes only about 5−10 min of annealing at 110 °C for PtBA to form a continuous surface wetting layer that is thick enough to make the underneath PS undetectable by XPS. Based on the known sampling depth of XPS, the thickness of the PtBA wetting layer must exceed 10 nm. Further annealing does not change the value of R_a. After rinsing with cyclohexane, samples were put into a vacuum oven and dried at room temperature. XPS survey and C_{1s} spectra were then recorded. Silicon peaks are not detected in the survey spectra, and analysis of the C_{1s} spectra indicates that R_a is still ~14%. The XPS results show that, upon annealing, a PtBA wetting layer forms at the air−polymer interface and that a second PtBA wetting layer also forms at the interface with the silicon wafer, underneath the PS droplets.

Consideration of surface and interfacial tension values provides a quantitative explanation for the observed morphology. The interfacial tension between PS and PtBA, γ_{12}, can be calculated using the harmonic mean equation:[19]

$$\gamma_{12} = \gamma_1 + \gamma_2 - 4\gamma_1^{d}\gamma_2^{d}/(\gamma_1^{d} + \gamma_2^{d}) - 4\gamma_1^{p}\gamma_2^{p}/(\gamma_1^{p} + \gamma_2^{p}) \quad (5)$$

where γ denotes surface tension and the subscripts 1 and 2 denote PS and PtBA, respectively. The superscripts p and d denote the polar and dispersive components of the surface tensions, respectively. Surface tension data for PS and PtBA are given in Table 4.

Equation 5 yields a value for the interfacial tension between PS and PtBa, γ_{12}, of about 1 mJ/m^2. With this value, $\gamma_1 > \gamma_{12} + \gamma_2$, and PtBA is expected to wet both PS and the silicon substrate. Conversely, PS is expected to dewet both PtBA and the silicon wafer during spin-coating or annealing. A PtBA wetting layer is therefore expected to form at both the air−polymer and the polymer−substrate interfaces, as is observed experimentally.

The interfacial and surface tension considerations, however, do not explain why the PS phases form droplets (Figure 17b) instead of one layer sandwiched between two PtBA layers as depicted in Figure 17c. It is interesting to note, however, that PS/poly(methyl methacrylate) (PMMA) blend thin films[6] also exhibit PS droplets after annealing at 190 °C for 40 min. Unfortunately, the authors did not perform selective dissolution or XPS measurement to fully understand details of the morphology of the annealed sample. PS/PMMA films are expected to behave differently from PS/PtBA films because PMMA does not have a lower surface tension than PS. Thus, in PMMA blends, PS droplets are not expected to be covered with a PMMA overlayer. The dynamics of annealing are also expected to differ for the two systems because PtBA has a much lower T_g than PMMA. Morphology changes due to annealing should therefore be much more rapid in the PS/PtBA system.

A more quantitative explanation for the stability of PS dispersed phases in annealed samples can be provided by consideration of the free energy per unit area of the blends and how it would vary with the size of PS droplets dispersed within the PtBA matrix. This model is appropriate for the annealed samples because they have reached a quasi-equilibrium state wherein droplet growth is extremely slow. In addition, we are not concerned here about the details of how the initial structure formed during spin-coating, but why the

morphology initially formed becomes arrested as PS droplets of finite size, even after long annealing times.

In the model, we consider that the PS domains are spherical phases embedded within a PtBA matrix, as shown in Figure 17b. Although the domains are not really spherical, this geometry requires only one parameter to describe the PS morphology, the domain radius, r, and thus represents the simplest treatment of the thin film free energy. If the film thickness, t, is larger than the diameter of PS droplets, the free energy F can be written as

$$F = \gamma_{12}(4\pi r^2 n) + \gamma_2 A \tag{6}$$

where n is the number of PS drops and A is the projected surface area of the thin film or the area of Si substrate. The first term on the right side of (6) is the interfacial energy between PS and PtBA, and the second term is the surface energy of the PtBA surface overlayer. The model assumes that all PS droplets are spherical in shape and of the same size. The substrate/polymer interfacial energy is neglected since it provides an identical free energy contribution for the two physical models that are to be compared (i.e., parts b and c of Figure 17).

If the average film thickness is smaller than the diameter of PS drops, the free energy is

$$F = \gamma_{12}(4\pi r^2 n) + \gamma_2 A + \gamma_2[2\pi r(2r - t) - \pi R^2] \tag{7}$$

The third term on the right-hand side of (7) is associated with the excess surface area created when PS droplets protrude out of the film surface. The parameter R defined in Figure 17b is

$$R^2 = r^2 - (r - t)^2 \tag{8}$$

Since PS droplets are totally encapsulated by PtBA, γ_2 is the appropriate surface tension to be used for the third term in (7).

The volume ratio of PS to PtBA is essentially equal to the mass ratio, m, in the original solution; therefore

$$m = \frac{n\frac{4}{3}\pi r^3}{At - n\frac{4}{3}\pi r^3} \qquad \text{for } t \geq 2r \tag{9}$$

$$m = \frac{n\frac{4}{3}\pi r^3}{At - n\frac{1}{6}\pi t[3R^2 + t^2]} \qquad \text{for } t \leq 2r \tag{10}$$

The small amount of PtBA that covers the protruding part of PS drops is also neglected here. The parameter α is defined as the ratio of the PS droplet radius, r, to the film thickness, t. If the amount of PtBA in the wetting layer covering PS were included, the parameter α would have finite practical limits that were dependent on the PS domain radius, making representation of the results more difficult. Solving eqs 6 and 9 and substituting for r with αt yields

$$F/A = \frac{3m\gamma_{12}}{m\alpha + \alpha} + \gamma_2 \qquad \text{for } \alpha \leq 0.5 \tag{11}$$

Similarly

$$F/A = \frac{4\gamma_{12}\alpha^3 + m[12\alpha^2(\gamma_{12} + \gamma_2) - 9\gamma_{12}\alpha + 2\gamma_{12}]}{4\alpha^3 + m(3\alpha - 1)} \qquad \text{for } \alpha \geq 0.5 \tag{12}$$

For the flat multiple layer model (Figure 18c) the free energy is simply

$$F/A = \gamma_2 + 2\gamma_{12} \tag{13}$$

The value of γ_2 for PtBA is 33.7 mJ/m^2, and γ_{12} between PtBA and PS was estimated earlier to be about 1 mJ/m^2.

The calculated free energy per unit area for the PS droplet model (for $m = 1$) is shown in Figure 18 as a function of α. The value of F/A calculated for the multiple-layer model is included in the figure for comparison. For clarification, the results are displayed separately for two ranges, $0 < \alpha < 9$ and $\alpha > 9$. The calculations illustrate that there is a local free energy trap for α values near 0.5 such that the system needs to overcome a free energy barrier to reach the predicted global equilibrium at infinite α. The kinetic trap or local minimum in free energy corresponds to the point at which the drop diameter is equal to the film thickness. Initially, F/A drops monotonically with increase of drop size due to a decrease in total interfacial area between PS and PtBA. When the droplet becomes larger than the film thickness, protrusion from the surface increases

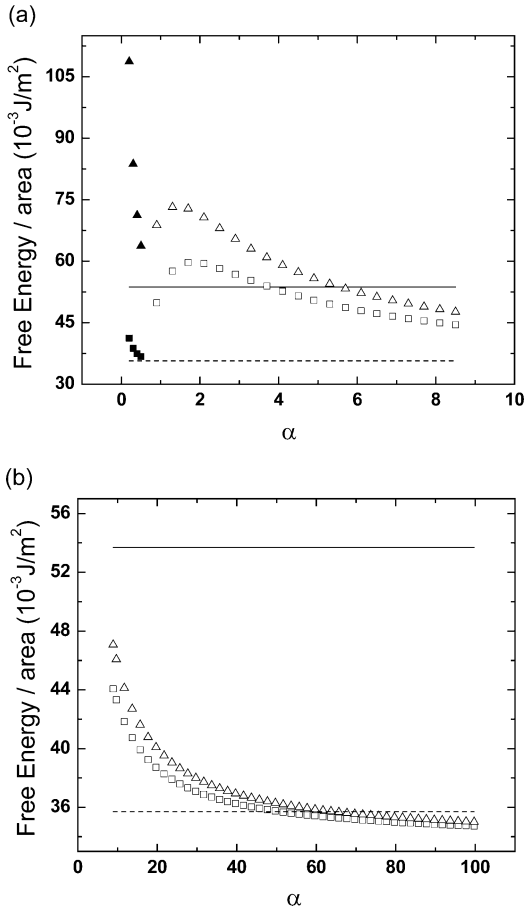

Figure 18. Calculation of free energy per area vs α: interface tension series. (a) $0 < \alpha < 9$; (b) $\alpha > 9$ (—, layer structure, $\gamma_{12} = 10$; - - -, layer structure, $\gamma_{12} = 1$; ▲, drop structure, $\gamma_{12} = 10$, $0 < \alpha < 0.5$; △, drop structure, $\gamma_{12} = 10$, $\alpha > 0.5$; ■, drop structure, $\gamma_{12} = 1$, $0 < \alpha < 0.5$; □, drop structure, $\gamma_{12} = 1$, $\alpha > 0.5$).

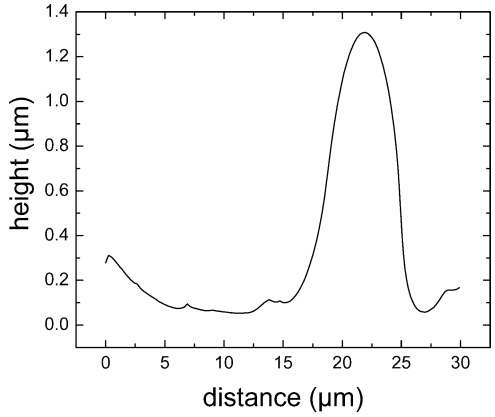

Figure 19. Typical line scan of an annealed sample.

the free surface area and thus the total free energy of the system up to the point where α reaches a value of about 1.7. Further increases in the drop diameter cause a monotonic decrease in free energy because the PS/PtBA interfacial energy contribution begins to dominate over the effects of the PtBA surface energy. The limiting morphology is a single drop of polystyrene encapsulated by a wetting layer of PtBA. For the compositions studied, experimental α values with magnitudes in the tens of thousands are possible if a 7−10 nm thick wetting layer (i.e., the sampling depth of XPS) is assumed to cover a single PS droplet.

The minimum *F*/*A* value for the droplet model becomes lower than that for the multiple layer structure at high α, providing a reasonable explanation for the stability of the droplet morphology upon annealing. The crossover occurs well within the range of possible experimental α values. The calculations are also consistent with the observed gradual growth in droplet size observed upon extended annealing. Figure 19 shows a representative NCM-AFM line scan for the sample shown in Figure 16a. Although the PS domains are not spherical, an effective radius can be estimated to be about 650 nm. The thickness of the base PtBA film is about 40 nm. The parameter α therefore has an experimental magnitude of the order of 15−20. According to the model calculations, this would exceed the α value of the kinetic trap; however, the model is crude and the PS domains are not spherical, so it is not clear what the value of α for the kinetic trap should really be. A more sophisticated model might provide better correspondence with the data; however, the local free energy minimum found in the crude model presented herein does furnish a qualitative explanation for the apparent stability and slow growth of the PS droplet morphology.

Figure 20 also illustrates how interfacial tension is predicted to affect the morphology. It is evident that *F*/*A* increases with the interfacial tension and that an increase in interfacial tension makes the drop structure more favorable. For example, at $\alpha = 52.1$, *F*/*A* for the drop structure is only 0.04 mJ/m^2 lower than that for the multiple layer structure when γ_{12} is 1 mJ/m^2. When γ_{12} is 10 mJ/m^2, *F*/*A* for the drop structure is 17.5 mJ/m^2 lower than that for the layer structure.

Figure 19 illustrates the effects of composition on *F*/*A*. The results show that the drop structure is always more energetically favorable than the multilayer structure for the composition range investigated. The energy barrier, associated with the increase in total surface area when the PS phase protrudes out of the film, increases with

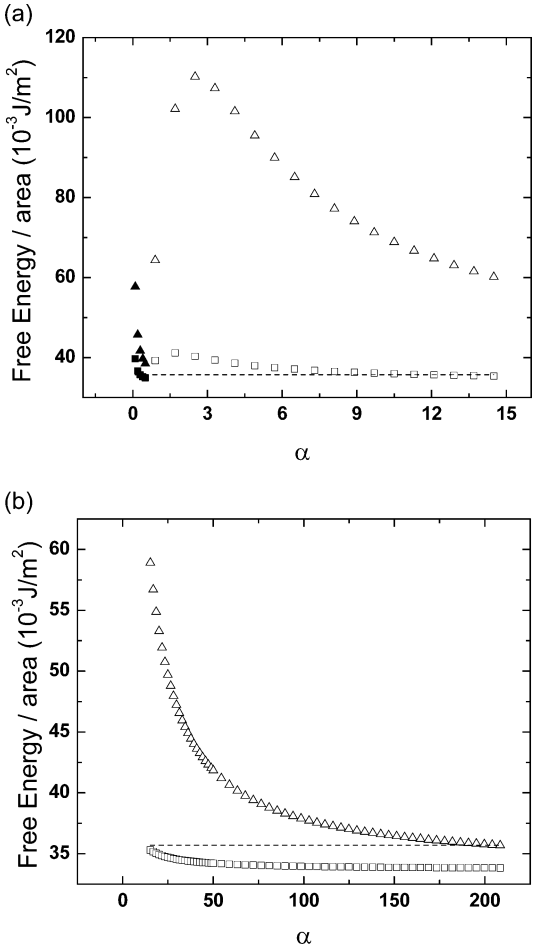

Figure 20. Calculation of free energy per area vs α: weight ratio series. (a) $0 < \alpha < 15$; (b) $\alpha > 15$ (- - -, layer structure; ▲, drop structure, PS:PtBA = 4:1, $0 < \alpha < 0.5$; Δ, drop structure, PS:PtBA = 4:1, $\alpha > 0.5$; ■, drop structure, PS:PtBA = 1:4, $0 < \alpha < 0.5$; □, drop structure, PS:PtBA = 1:4, $\alpha > 0.5$).

the ratio of PS to PtBA. The local free energy minimum found in the simple model provides a reasonable explanation why the PS domains form stable droplets, even after long annealing times.

Summary

The effect of spin-coating conditions on the morphologies of thin films is studied for blends of PS with PtBA. In all cases, the films exhibit laterally phase-separated morphologies wherein the thickness of PS domains is greater than that of the PtBA domains. The morphology progresses from PS islands to PTBA holes as the composition of PS in the blend increases when the film thickness is in the range 58−227 nm. A networklike PS domain structure is observed for lower film thicknesses. The thicknesses of both the PS and PtBA regions show a linear increase with concentration of the spin-coating solution for thicker films, and the diameter of PtBA holes increases monotonically with thickness. Addition of P(S-*b*-tBA) diblock copolymer decreases the size of PtBA holes and thus is an effective means for modifying thin film morphology. Upon annealing, PS droplets form that become completely encapsulated by PtBA and tend to coalesce only slowly with increased annealing time. A free energy model is developed that accounts for the stability of the PS droplet morphology and how it changes upon annealing. The model illustrates that the surface tension of PtBA and the interfacial tension

between PS and PtBA are the two crucial parameters that control the domain structures observed in thin films of polymers prepared by spin-coating.

Acknowledgment. This material is based on work supported by, or in part by, the US Army Research Office and Grant DAAD19-00-1-0104 and was supported in part by the MRSEC Program of the National Science Foundation under Award DMR-0213574.

References and Notes

(1) See for example: (a) Paul, D. R., Bucknall, C. B., Eds.; *Polymer Blends*; Wiley: New York, 2000. (b) Paul, D. R.; Newman, S. *Polymer Blends*; Academic Press: New York, 1978. (c) Datta, S.; Lohse, D. J. *Polymeric Compatibilizers: Uses and Benefits in Polymer Blends;* Hanser-Gardner: Cincinnati, OH, 1996.
(2) Hall, D. B.; Underhill, P.; Torkelson, J. M. *Polym. Eng. Sci.* **1998**, *38*, 2039.
(3) Schubert, D. W.; Dunkel, T. *Mater. Res. Innovations* **2003**, *7*, 314.
(4) Walheim, S.; Böltau, M.; Mlynek, J.; Krausch, G.; Steiner, U. *Macromolecules* **1997**, *30*, 4995.
(5) Ton-That, C.; Shard, A. G.; Daley, R.; Bradley, R. H. *Macromolecules* **2000**, *33*, 8453.
(6) Ton-That, C.; Shard, A. G.; Teare, D. O. H.; Bradley, R. H. *Polymer* **2001**, *42*, 1121.
(7) Ton-That, C.; Shard, A. G.; Bradley, R. H. *Polymer* **2002**, *43*, 4973.
(8) Tanaka, K.; Takahara, A.; Kajiyama, T. *Macromolecules* **1996**, *29*, 3232.
(9) Wang, H.; Composto, R. J. *Phys. Rev. E* **2000**, *61*, 1659.
(10) Wang, H.; Composto, R. J.; Hobbie, E. K.; Han, C. C. *Langumir* **2001**, *17*, 2857.
(11) Wang, H.; Composto, R. J. *Macromolecules* **2002**, *35*, 2799.
(12) Sprenger, M.; Walheim, S.; Budkowski, A.; Steiner, U. *Interface Sci.* **2003**, *11*, 225.
(13) Yuan, C.; Ouyang, M.; Koberstein, J. T. *Macromolecules* **1999**, *32*, 2329.
(14) Qu, S.; Darke, C. J.; Liu, Y.; Rafailovich, M. H.; Sokolov, J.; Phelan, K. C.; Krausch, G. *Macromolecules* **1997**, *30*, 3640.
(15) Hoppe, H.; Heuberger, M.; Klein, J. *Phys. Rev. Lett.* **2001**, *86*, 4863.
(16) Wang, H.; Composto, R. J. *Interface Sci.* **2003,** *11*, 237.
(17) Rigby, D.; Lin, J. L.; Roe, R. J. *Macromolecules* **1985**, *18*, 2269.
(18) Hu, W.; Koberstein, J. T.; Lingelser, J. P.; Gallot, Y. *Macromolecules* **1995**, *28*, 5209.
(19) Wu, S. *Polymer Interface and Science;* Marcel Dekker: New York, 1982; Chapters 2−4.
(20) Adão, M. H.; Saramago, B.; Fernandes, A. C. *J. Colloid Interface Sci.* **1999**, *217*, 94.

MA049664+